

REFERENCES

1. Greskovich,C., and Rosoloedki, J.H. Sintering of covalent. J.Am.Ceram.Soc. 59 (Jul.-Aug. 1976) : 336-343.
2. Kleebe, H. Structure and chemistry of interfaces in Si_3N_4 ceramics studied by transmission electron microscopy. J.Am.Ceram.Soc.Jap. 105 (1997) : 490-510.
3. Wills,R.R. Silicon Yttrium Oxyynitrides. J.Am.Ceram.Soc. 57 (October 1974) : 459.
4. Diane M., Mieskowski, and William A. Sanders. Oxidation of silicon nitride sintered with rare-earth oxide additions. J.Am.Ceram.Soc. 68 (July 1985) : C-160-C-163.
5. Jian-Feng Yang, Tatsuki Ohji, and Koichi Niihara. Influence of Yttria-Alumina content on sintering behavior and microstructure of silicon nitride ceramics. J.Am.Ceram.Soc. 83 (August 2000) : 2094-2096.
6. Gauckler, L.J., Hohnke, H., and Tien, T.Y. The system Si_3N_4 - SiO_2 - Y_2O_3 . J.Am.Ceram.Soc. 63 (Jan.-Feb. 1980) : 35-37.
7. Frederick, F. Lange. Fabrication and properties of dense polyphase silicon nitride. J.Am.Ceram.Bull. 62 (1983) : 1369-1374.
8. Akihiko Tsuge., Nishida, K., and Komatsu, M. Effect of crystallizing the grain boundary glass phase on the high-temperature strength of Hot-Pressed Si_3N_4 containing Y_2O_3 . J.Am.Ceram.Soc. 58 (Jul.-Aug. 1975) : 323-326.
9. Wills, R.R. Reaction of Si_3N_4 with Al_2O_3 and Y_2O_3 . J.Am.Ceram.Soc. 58 (Jul.-Aug. 1975) : 335.
10. Lange, F.F. Relation between strength, Fracture Energy and microstructure of Hot-Pressed Si_3N_4 . J.Am.Ceram.Soc. 56 (October 1973) : 518-522.
11. Tsuge, A., Kudo, H., and Komeya, K. Reaction of Si_3N_4 and Y_2O_3 in Hot-Pressing. J.Am.Ceram.Soc. 59 (June 1977) : 269-270.
12. John, A. Mangels, and Gerald J. Tennenhouse. Densification of Reaction-Bonded silicon nitride. J.Am.Ceram.Bull. 59 (1980) : 1216-1218.
13. John A., Mangels, and Gerald, J. Tennenhouse. Sintering behavior and microstructure development of Yttrium-Doped reaction-bonded silicon nitride. J.Am.Ceram.Bull. 60 (1981) : 1306-1310.
14. Priest, H.F., Priest, G.L., and Gazza, G.E. Sintering of Si_3N_4 under high nitrogen

- pressure. J.Am.Ceram.Soc. 60 (Jun.-Feb. 1977) : 81.
15. Greskovich, C. Preparation of high density Si_3N_4 by gas pressure sintering process. J.Am.Ceram.Soc. 64 (December 1981) : 725-730.
 16. Sunil Dutta. Fabrication, microstructure, and strength of sintered β' Si_3N_4 solid solution. J.Am.Ceram.Bull. 59 (December 1980) : 623-25,634.
 17. Lee, H.R., Lee, C.J., and Deug J. Kim. Effect of α - Si_3N_4 powder bedding on the microstructure of gas pressure sintered Si_3N_4 ceramics. Materials Letters. 52 (2002) : 355-359.
 18. Kazushige Yokoyama, et al. Solid-gas reaction during sintering of Si_3N_4 ceramics (Part 1). J.Am.Ceram.Soc.Jap. 108 (2002) : 6-9.
 19. Kazushige Yokoyama, et al. Solid-gas reaction during sintering of Si_3N_4 ceramics (Part 3). J.Am.Ceram.Soc.Jap. 108 (2002) : 230-235.
 20. Kazushige Yokoyama, et al. Solid-gas reaction during sintering of Si_3N_4 ceramics (Part 4). J.Am.Ceram.Soc.Jap. 108 (2002) : 357-364.
 21. Shigetaka Wada. Control of instability of Si_3N_4 during pressureless sinterng. J.Am.Ceram.Soc.Jap. 109 (2001) : 803-808.
 22. Shigetaka Wada, et al. Sintering of Si_3N_4 ceramics in air atmosphere furnace. J.Am.Ceram.Soc.Jap. 109 (2001) : 281-283.
 23. Naoto Hirosaki, et al. New ceramics based on silicon nitride[Online]. (n.d.). Available form: <http://sakimori.nims.go.jp/oneday2000/ceramis.html> [2002, June 8]
 24. Shinroku Saito, ed. Fine ceramics. New York : Elsevier Science Publishing, 1985.
 25. Frank L. Riley. Silicon nitride and related materials. J.Am.Ceram.Soc. 83 (February 2000) : 245-265.
 26. Yet-Ming Chiang, Dunbo birnic III, w. David Kingery. Physical ceramics. New York : John Wile & Sons, 1997.
 27. Pezzotti, G. et al. Growth isotherms of liquid-phase sintered silicon nitride. J.Am.Ceram.Soc.Jap. 105 (1997) : 691.
 28. Xin Xu, Liping Huang, Xuejian Liu, Xiren Fu. Effects of α/β ratio in starting powder on microstructure and mechanical properties of silicon nitride ceramics.

- Ceramics International. 28 (2002) : 279-281.
29. Wotting, G., Ziegler, G. Powder characteristics and sintering behavior of Si_3N_4 -powders. Interceram. 35 (1986)
30. Hirotsuru, H. et al. Influence of phase transformation on densification behavior and grain growth of fine silicon nitride powder. J.Am.Ceram.Soc.Jap. 104 (1995) : 24-28.
31. Greskovich, C., and Prochazka, S. Stability of Si_3N_4 and liquid phase(s) during sintering. J.Am.Ceram.Soc.Jap. (July 1981) : C-96-C-97.
32. Standard test methods for apparent porosity, liquid absorption, apparent specific gravity, and bulk density of refractory shapes by vacuum pressure. Annual book of ASTM standards. 15.01, 14.02 (February 1993) : 137-140.
33. Charles, P., Gazzara, and Donald R. Messier. Determination of phase content of Si_3N_4 by X-Ray diffraction analysis. J.Am.Ceram.Bull. 56 (1977) : 777-780.
34. Shigetaka Wada. Increase of oxygen content in Si_3N_4 powder during ball milling using alcohol as solvent. J.Am.Ceram.Soc.Jap. 104 (1996) : 1092-1094.
35. Hyati, M.J., and Day, D.E. Glass properties in the Yttria-Alumina-Silica system. J.Am.Ceram.Soc. 70 (1987) : C-283-C-287.
36. Hirosaki, N., and Matsubara, H. Effect of heat treatment of Si_3N_4 on grain growth behavior and grain boundary structure. J.Am.Ceram.Soc.Jap. 105 (1996) : 234-238.
37. Kazusige Yokoyama, and Shigetaka Wada. Solid-gas reaction during sintering of Si_3N_4 ceramic (Part 5). J.Am.Ceram.Soc.Jap. 108 (2000) : 627-632.
- Testing method for toughness of high performance ceramic (JIR r 1607). 1995.
- Testing method for Vickers hardness of high performance ceramic (JIS R 1610). 1991.
40. Standard test method for biaxial flexure strength (Modus of rupture) of ceramic substrates. American national standard (ANSI / ASTM F394-398). : 780-787.
41. Bongkoch Piempermpoon. Improvement of thermal conductivity of alumina for peltier element. Master's Thesis, Department of Material Science. Chulalongkorn University, 2002.
42. Hiroshi Yamashita and Akira Yamaguchi. Oxidation of Aluminum Oxynitride-Boron

- nitride (ALON-BN) composite prepared by reaction sintering.
J.Am.Ceram.Soc.Jap. 109 (2001) : 94-99.
43. Kazusige Yokoyama, and Shigetaka Wada. Solid-gas reaction during sintering of Si_3N_4 ceramic (Part 5). J.Am.Ceram.Soc.Jap. 108 (2000) : 627-632.
44. Michel W. Barsoum. Fundamentals of ceramics. International Editions. New York : McGraw-Hill Companies, 1977.
45. Hill, R., Osgood R.M., Sakaki. Jr. H., Zunger, A. Ceramics mechanical properties failure behabior, materials selection. New York : Springer-Verlag Berlin Heidelberg, 1998 : 34-37.
46. JANAF Thermochemical Table,2d ed. U.S. Government printing office, Washington DC., 1971



Appendices

ศูนย์วิทยทรัพยากร
จุฬาลงกรณ์มหาวิทยาลัย

APPENDIX A

Table A-1 Properties of Si_3N_4 (1)

Type	SN-7	SN-E10
Alpha -phase (%)	74	95
Chemical composition (%)	Si = 59 N = 38 Fe = 0.3 Al = 0.2 Ca = 0.2 Mg = <0.1 O = 1.6	- - Fe = < 100 ppm Al = trace Ca = trace - O = < 2.0 Cl = < 100 ppm
Specific surface area (m^2/g)	4	9-13

Table A-2 Properties of Si_3N_4 (2)

Type	SN-KO5	SN-F2
Alpha -phase (%)	≥ 80	< 1
Chemical composition	N = 38.8 Fe \leq 300 (ppm) Al \leq 500 (ppm) Ca \leq 100 (ppm) Cl \leq 100 (ppm) O = 0.62	Free Si < 0.5 (%) - Fe = 0.2 (%) Al = 0.1 (%) Ca = 0.1 (%) - O = < 2.0 Cl = < 100 ppm
Specific surface area (m^2/g)	4.0 ~ 6.0	1
Size of crystal (μm)	-	29

* Analyzed oxygen content was 1.29 mass %

Table A-3 Properties of Al_2O_3 used as packing powders

Qualitative data / Grade		AKP-30	A-11	AM-21
Chemical composition	L.O.I (%)		0.01	0.05
	Fe_2O_3 (%)		0.01	0.01
	SiO_2 (%)		0.01	0.02
	Na_2O (%)		0.30	0.26
	Al_2O_3 (%)	99.99	99.7	99.7
	H_2O (%)		0.06	0.10
Physical composition	True specific gravity		3.93	3.95
	Apparent specific gravity			
	Packed bulk density (g/cm^3)		-	1.30
	Loose bulk density (g/cm^3)		-	0.70
	Mean particle size (μm)		63	4.0
	Specific surface area (m^2/g)		150	-
	Pore volume (cm^3/g)		0.30	-

ศูนย์วิทยทรัพยากร
จุฬาลงกรณ์มหาวิทยาลัย

Table A-4 Properties of Y_2O_3 used as an additive

Properties	Details
Chemical composition (%)	$\text{Y}_2\text{O}_3 = 99.9$ $\text{CaO} = 0.0007$ $\text{Al}_2\text{O}_3 = 0.001$ $\text{Fe}_2\text{O}_3 = 0.001$ $\text{SiO}_2 = 0.0087$
Specific surface area (m^2/g)	29.9
Size of crystal (μm)	4.6

Table A-5 Properties of Al_2O_3 used as an additive

Qualitative data / Grade		AKP-30
Purity	Al_2O_3 (%)	99.99
Impurity Level	Fe (ppm)	≤ 20
	Si (ppm)	≤ 40
	Na (ppm)	≤ 10
	Mg (ppm)	≤ 10
	Cu (ppm)	≤ 10
Packed bulk density (g/cm^3)		1.1~1.5
Loose bulk density (g/cm^3)		0.7~1.1
Particle size (μm)		0.4~0.6
Specific surface area (m^2/g)		4-6

APPENDIX B**Table B-1** The temperature inside and outside of the crucible

T (°C)	T ₁ (Back) (mV)	T ₂ (Top) (mV)	T (°C)	T ₁ (Back) (mV)	T ₂ (Top) (mV)	T (°C)	T ₁ (Back) (mV)	T ₂ (Top) (mV)
29	0.00	0.00	1154	6.02	3.80	1600	10.93	10.90
106	0.10	0.00	1205	6.52	4.20	1600	10.93	10.90
156	0.10	0.00	1255	7.04	4.70	1600	10.93	10.90
204	0.10	0.00	1305	7.58	5.10	1600	10.93	10.90
251	0.26	0.00	1353	8.11	5.70	1600	10.93	10.90
307	0.37	0.08	1411	8.75	6.30	1600	10.93	10.90
353	0.52	0.10	1452	9.18	6.70	1600	10.93	10.90
408	0.70	0.20	1525	10.04	7.60	1600	10.93	10.90
453	0.88	0.20	1561	10.45	8.00	1600	10.93	10.90
483	1.10	0.30	1602	10.94	8.60	1600	10.93	10.90
556	1.35	0.50	1601	10.94	9.20	1600	10.93	10.90
601	1.62	0.60	1600	10.94	9.60	1600	10.93	10.90
656	1.95	0.80	1600	10.94	10.00	1548	10.34	10.90
703	2.23	0.90	1600	10.94	10.30	1419	8.84	10.80
754	2.56	1.10	1600	10.94	10.50	1324	7.91	10.40
805	2.98	1.40	1600	10.94	10.60	1268	7.17	9.90
853	3.31	1.60	1600	10.94	10.70	1212	6.61	9.30
906	3.76	1.90	1600	10.94	10.80	1154	6.03	8.60
949	4.11	2.20	1600	10.94	10.80	1109	5.58	8.00
1003	4.60	2.60	1600	10.94	10.80	1067	5.16	7.50
1056	5.06	3.00	1600	10.93	10.80	1023	4.79	6.90
1108	5.54	3.40	1600	10.93	10.90	986	4.43	6.40

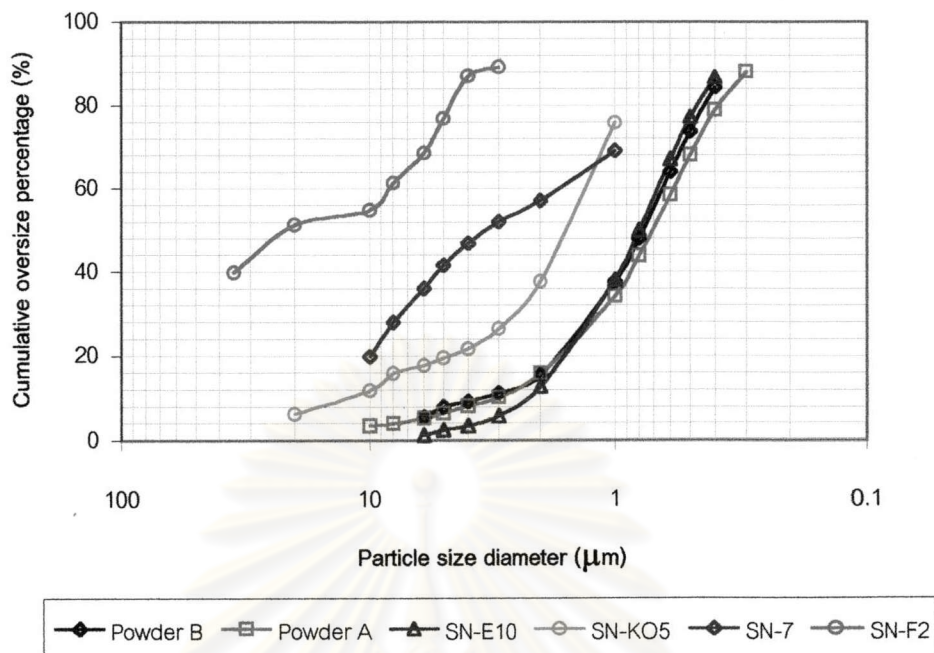


Fig B-1 Particle size distribution of Si_3N_4 powders

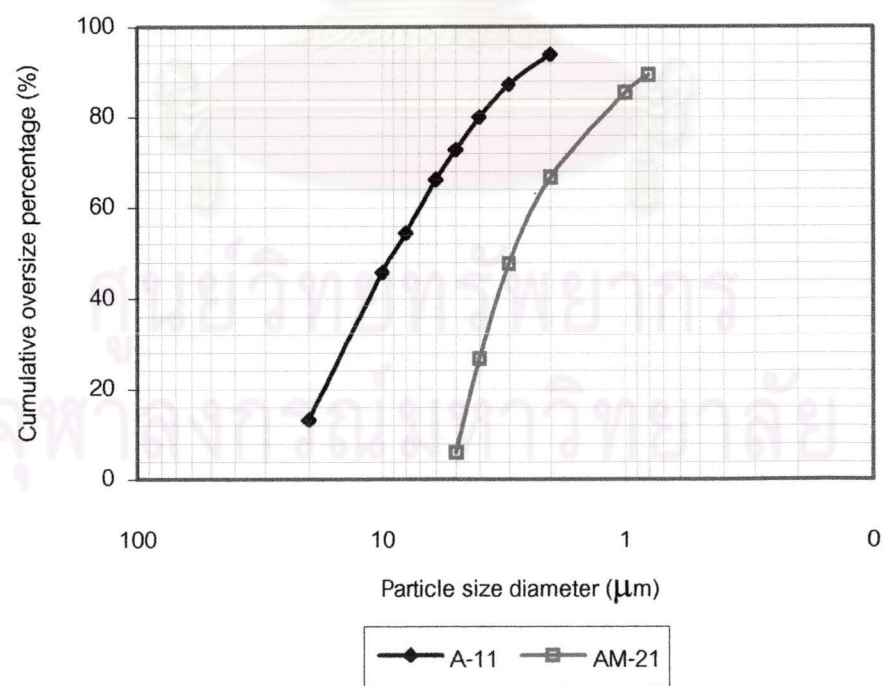


Fig B-2 Particle size distribution of Al_2O_3 packing powders

Table B-2 Particle size of SN-F2 packing powder measured by sieve analysis

NO. of sieve (mesh)	Particle size (μm)	Weight ratio (%)	Accumulate weight (%)
#50	300	0.00	0.00
#100	150	0.15	0.32
#140	106	4.52	9.59
#200	75	16.11	34.20
#325	45	32.11	68.16
Pan	-45	47.11	100.00

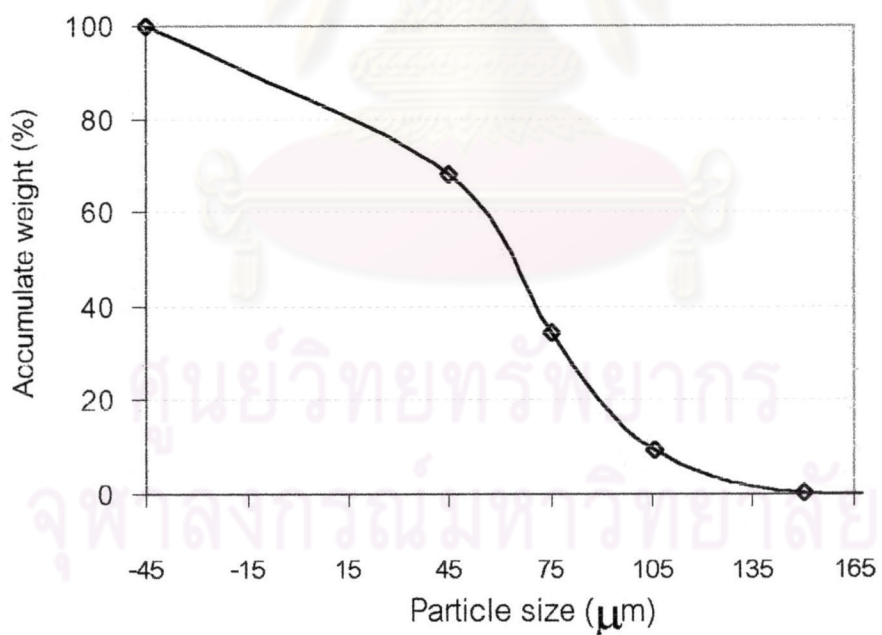
**Fig B-3** Relationship between weight ratio and particle size of SN-F2 powder by sieve analysis

Table B-3 Features of packing powder after sintering for mixed powder A

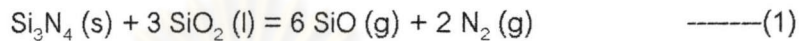
Condition No.	Packing powder	Conglomerate		Oxide layer	surface occur		Color	Shrinkage	Lid stick	stick to crucible					
		Strong	Loose	Thick	Thin	Glass	Bubble	Crack	Gray	Creamy	White	large	Little	Strong	Little
C1	SN-7 1550, 5 °C/min	o							o				o	o	
C2			o							o		o	o	o	o
C3		o									o	o		o	o
C4	SN-7 (10% BN) 1550, 5 °C/min		o					o	o				o		
C5		o		o		o	o	o	o			o	o	o	o
C6			o					o	o	o		o	o	o	o
C7	SN-7 (10% BN) 1600, 5 °C/min	o		o	o	o	o	o				o	o	o	
C8			o							o		o	o		o
C9		o		o	o	o	o	o				o	o	o	
C10	SN-7 (10% BN) 1600, 10 °C/min		o		o				o			o	o	o	o
C11		o		o	o	o	o	o				o	o	o	o
C12			o	o	o				o			o	o	o	o
C13	SN-7 (10% BN) 1700, 10 °C/min	o								No data.					
			o		o					o		o	o	o	o
		o									o	o	o	o	o

Table B-4 Features of packing powder after sintering for mixed powder B

APPENDIX C

Calculation of equilibrium $P_{\text{SiO}}(\text{g})$ as a function of temperature

In the previous work, it has been reported that the mass loss of Si_3N_4 during sintering comes from the reaction between Si_3N_4 (s) and SiO_2 (l) according to reaction (1).²¹⁾



The equilibrium constant of the reaction, K_p , is calculated from the equation (2).⁴⁴⁾

$$K_p = \frac{P_{\text{SiO}}^6 \cdot P_{\text{N}_2}^2}{a_{\text{Si}_3\text{N}_4(\text{s})} \cdot a_{\text{SiO}_2(\text{l})}} \quad \text{-----(2)}$$

As the activity of a solid and liquid is 1.⁴⁴⁾ Thus, the activity of Si_3N_4 , ($a_{\text{Si}_3\text{N}_4(\text{s})}$) and SiO_2 , ($a_{\text{SiO}_2(\text{l})}$) is 1. Then:

$$K_p = P_{\text{SiO}(\text{g})}^6 \cdot P_{\text{N}_2(\text{g})}^2 \quad \text{-----(3)}$$

From equation (3), the partial pressure of the SiO that is in equilibrium of equation (1) is determined by equation (4):

$$\Delta G = \Delta G^\circ + RT \ln K_p \quad \text{-----(4)}$$

The other extreme occurs when the driving force for the reaction is zero, that is

$\Delta G = 0$ then :

$$0 = \Delta G^\circ + RT \ln K_p$$

$$\ln K_p = -(\Delta G^\circ / RT)$$

$$\log K_p = \frac{-\Delta G^0}{2.302RT}$$

$$\log K_p = \frac{-\Delta G^0}{4.576T} \quad \text{---(5)}$$

As equation (6), ΔG^0 is the free energy changes that calculate form the free energy of each compound i (ΔG_i^0). All ΔG_i^0 of each compound, which is Si_3N_4 (s), Si (l), N_2 (g) and Si (g)), are seen in the JANAF thermodynamic Table.⁴⁶⁾

$$\Delta G = \Delta G_i^0(\text{products}) - \Delta G_i^0(\text{reactants}) \quad \text{---(6)}$$

In this case, assuming Partial pressure of N_2 gas, $P_{\text{N}_2(g)}$ is approximate 0.8 atm, because air includes 80 % of nitrogen.²⁴⁾ And $R = 1.9872 \text{ Kcal.mol}^{-1}\text{.K}^{-1}$ is used.⁴⁴⁾

Partial pressure of SiO gas, $P_{\text{SiO}(g)}$ calculate from take equation (3) into equation (5) Thus:

$$\log P_{\text{SiO}(g)}^6 \cdot P_{\text{N}_2(g)}^2 = \frac{-\Delta G^0}{4.576T}$$

$$\log P_{\text{SiO}(g)}^6 + \log P_{\text{N}_2(g)}^2 = \frac{-\Delta G^0}{4.576T}$$

$$6 \log P_{\text{SiO}(g)} = \frac{-\Delta G^0}{4.576T} - 2 \log (0.8)$$

$$\log P_{\text{SiO}(g)} = \left(\frac{\frac{1}{4.576T} \times (-\Delta G^0 + 0.88T)}{6} \right)$$

$$P_{\text{SiO}(g)} = 10^{\left(\frac{1}{27.45T} \times (-\Delta G^0 + 0.88T) \right)}$$

The dependence of $P_{\text{SiO}} \text{ (g)}$ upon the temperature describes by plot graph of the $P_{\text{SiO}} \text{ (g)}$ calculation result versus temperature as show in Table 1. (This experimental was investigated on temperature range 1873°C to 2023°C .) In addition, The relationship between temperature ($^{\circ}\text{C}$) and $P_{\text{SiO}} \text{ (g)}$ is shown in Fig 1.

Table 1 Calculation results of siliconoxide vapor pressures, P_{SiO} (g) in equilibrium over Si_3N_4 at on temperature range 1600°C to 1800°C (1873 K to 2073 K)

T ($^{\circ}\text{C}$)	T (K)	ΔG_i° (Kcal / mole)				ΔG° (Kcal/mole)	$P_{\text{SiO} \text{ (g)}}$ (MPa)
		$\text{Si}_3\text{N}_4 \text{ (s)}$	$\text{SiO}_2 \text{ (l)}$	SiO(g)	$\text{N}_2 \text{ (g)}$		
1600	1873	-26.922	-137.571	-59.935	0.000	80.025	0.003
1650	1923	-22.054	-135.262	-60.491	0.000	64.894	0.006
1700	1973	-16.803	-132.961	-61.043	0.000	49.432	0.013
1750	2023	-12.347	-130.666	-61.593	0.000	34.787	0.025
1800	2073	-7.124	-128.376	-62.139	0.000	19.418	0.049

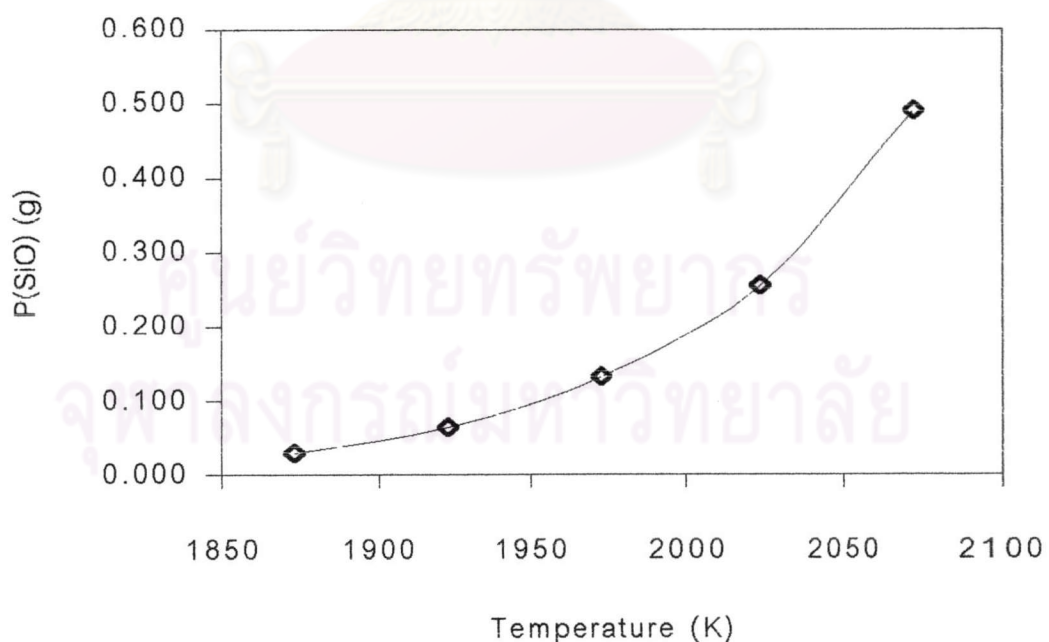


Fig 1 Relationship between partial pressure of SiO (g) and temperature (K)

APPENDIX D**Table D-1** Mass change, Bulk density and relative density of powder A specimens.

Code	Conditions					Sample No.	Mass change (%)	Bulk density (%)	Relative density (%)				
	T (°C)	Rate (°C/min)	Soaking (h)	Packing powders									
				Si ₃ N ₄	Al ₂ O ₃								
C1	1550	5	2	SN-7	AM-21	1	0.71	2.49	75.91				
				BN		2	0.75	2.52	76.73				
C2	1550	5	2	SN-E10	AM-21	1	-0.43	2.41	73.47				
						2	0.27	2.39	72.73				
C3	1550	5	2	SN-7	A-11	1	-0.46	2.60	79.28				
				BN		2	0.31	2.61	79.68				
C4	1550	5	2	SN-E10	A-11	1	0.10	2.42	73.89				
						2	2.40	2.47	75.19				
C5	1600	5	2	SN-7	A-11	1	0.61	2.76	84.28				
				BN		2	0.75	2.77	84.44				
C6	1600	5	2	SN-E10	A-11	1	-0.99	2.81	85.56				
						2	-0.38	2.76	84.15				
C7	1600	10	2	SN-7	A-11	1	0.20	2.71	82.62				
				BN		2	1.23	2.71	82.53				
C8	1600	10	2	SN-E10	A-11	1	-0.92	2.83	86.18				
						2	-0.41	2.84	86.50				
C9	1650	10	2	SN-7	A-11	1	0.24	2.86	86.59				
				BN		2	0.48	2.74	83.54				
C10	1650	10	2	SN-E10	A-11	1	-0.74	2.94	89.63				
						2	-1.91	2.97	90.55				
C11	1700	10	1	SN-7	A-11	1	0.31	2.84	86.59				
				BN		2	0.53	2.84	86.59				
C12	1700	10	1	SN-E10	A-11	1	-0.32	2.94	89.63				
						2	-1.09	2.96	90.24				
C13	1700	10	2	SN-E10	A-11	1	-0.12	2.96	90.24				
						2	-0.68	3.02	92.07				

Table D-2 Mass change, Bulk density and relative density of powder B specimens.

Code	Conditions					Lot No.	Mass change (%)	Bulk density (%)	Relative density (%)				
	T (°C)	Rate (°C/min)	Soaking (h)	Packing powders									
				Si ₃ N ₄	Al ₂ O ₃								
E1	1650	10	2	SN-KO5	A-11	1	-0.20	3.10	95.09				
						2	-0.72	3.08	94.48				
E2	1650	10	2	SN-F2	A-11	1	-1.56	3.15	96.63				
						2	-1.49	3.15	96.63				
E3	1700	10	2	SN-KO5	A-11	1	-0.59	3.11	95.40				
E4	1700	10	2	SN-F2	A-11	1	-0.52	3.12	95.71				
E5	1700	10	2	SN-KO5	A-11	2	-0.28	3.12	95.71				
E6	1700	10	2	SN-F2	A-11	2	-0.96	3.16	96.93				
E7	1700	10	2	SN-KO5	A-11	1	-1.97	3.14	93.32				
E8	1700	10	2	SN-F2	A-11	1	-1.44	3.16	93.93				
E9	1700	10	2	SN-KO5	A-11	2	-0.95	3.15	96.93				
E10	1700	10	2	SN-F2	A-11	2	-0.49	3.18	97.55				



APPENDIX E**Table E-1** Alpha content (%) in packing powder of powder A experiment

Temperature (°C)	Alpha content (%)				Alpha content (%)			
	SN-7+ 10 mass % BN				SN-E10			
	Top Bubble	Top	Bottom	No Layer	Top bubble	Top	Bottom	No Layer
1600 (5 °C/min)	-	78.9	72.1	-	-	-	-	-
1600 (10 °C/min)	-	71.7	82.6	-	-	-	-	100
1650 (10 °C/min)	87.7	70.9	61.1	-	-	100	100	-
1700, 1 h (10 °C/min)	-	80.0	75.9	-	-	94.9	96.4	-
1700, 2 h (10 °C/min)	-	-	-	-	-	-	-	95.4

Table E-2 Alpha content (%) in packing powder of powder B experiment

Temperature (°C)	Alpha Content (%)		Alpha Content (%)	
	SN-KO5		SN-F2	
	Top	Bottom	Top	Bottom
1650 (10 °C/min)	69.7	79.8	4.9	2.5
1700, 1 h (10 °C/min)	73.3	78.1	5.7	2.8
1700, 2 h (10 °C/min)	73.3	75.8	3.5	2.3

Table E-3 Crystal phase in SN-E10 and SN-7 packing powders after sintering

Type		Raw mat.	5 ⁰ C/min 1600 ⁰ C	10 ⁰ C/min 1600 ⁰ C	10 ⁰ C/min 1650 ⁰ C	10 ⁰ C/min 1700 ⁰ C	10 ⁰ C/min 1700 ⁰ C
SN-E10	Top	α	$\alpha + X_1$	-	$\alpha + X_1$	$\alpha + \beta + X_1$	$\alpha + \beta$
	Bottom				α	$\alpha + \beta$	
SN-7		$\alpha + \beta$	-	-	-	-	-
SN-7+BN	Glassy phase	$\alpha + \beta + BN$			$\alpha + \beta + BN$		
	Top		$\alpha + \beta + BN + X_1$	$\alpha + \beta + BN$	$\alpha + \beta + BN$	$\alpha + \beta + BN$	-
	Bottom		$\alpha + \beta + BN$	$\alpha + \beta + BN$	$\alpha + \beta + BN$	$\alpha + \beta + BN$	-

Table E-4 Crystal phase in SN-F2 and SN-KO5 packing powders after sintering

Type		10 ⁰ C/min, 1650 ⁰ C, 2 h	10 ⁰ C/min, 1700 ⁰ C, 1 h	10 ⁰ C/min, 1700 ⁰ C, 2 h
SN-F2	Top surface	$\beta + X_1 + X_2$	$\beta + X_1 + X_2$	$\beta + X_2$
	Bottom surface	β	β	$\beta + X_2$
SN-KO5	Top surface	$\alpha + \beta + X_1$	$\alpha + \beta + X_1$	$\alpha + \beta + X_1$
	Bottom surface	$\alpha + \beta$	$\alpha + \beta$	$\alpha + \beta$

Note: X_1 = Cristobalite

X_2 = Sinoite, Si_2N_2O

Table E-5 Alpha content (%) in specimens of powder A experiment

Temperature (°C)	Alpha content (%)		Alpha content (%)	
	SN-7+ 10 mass % BN		SN-E10	
	5 °C/min	10 °C/min	5 °C/min	10 °C/min
1550, 2 h	20.9	-	94.9	-
1550, 2 h	-	92.4	-	78.3
1600, 2 h	48.9	-	82.2	-
1600, 2 h	-	60.6	-	71.8
1650, 2 h	-	21.6	-	48.3
1700, 1 h	-	30.1	-	34.9
1700, 2 h	-	-	-	20.9

Table E-6 Alpha content (%) in specimens of powder B experiment

Temperature (°C)	Alpha Content (%)		Alpha Content (%)	
	SN-KO5		SN-F2	
	Lot 1	Lot 2	Lot 1	Lot 2
1650, 2 h (10 °C/min)	48.5	-	34.3	30.5
1700, 1 h (10 °C/min)	48.2	52.4	40.9	39.3
1700, 2 h (10 °C/min)	25.8	25.2	14.5	18.5

Table E-7 Crystal phase in Mixed powder A specimens

Powder packing		5 ⁰ C/min, 1550 ⁰ C, 2 h.	5 ⁰ C/min, 1600 ⁰ C, 2 h.	10 ⁰ C/min, 1600 ⁰ C, 2 h.	10 ⁰ C/min , 1650 ⁰ C, 2 h.	10 ⁰ C/min, 1700 ⁰ C	
						1 h.	2 h.
Sintering with SN-7	SN-E10 Crucible	$\alpha+\beta$	-	-	-	-	-
	SN-7 Crucible	$\alpha+\beta$	-	-	-	-	-
Sintering with SN-7 + BN	SN-E10 Crucible	$\alpha+\beta$	$\alpha+\beta$	$\alpha+\beta$	$\alpha+\beta$	$\alpha+\beta$	$\alpha+\beta+x_2$
	SN-7 Crucible	$\alpha+\beta$	$\alpha+\beta$	$\alpha+\beta$	$\alpha+\beta$	$\alpha+\beta$	-

Table E-8 Crystal phase in Mixed powder B specimens

Temperature (⁰ C)	Sintering with SN-KO5 packing powder		Sintering with SN-F2 packing powder	
	Lot 1	Lot 2	Lot 1	Lot 2
10 ⁰ C/min, 1650 ⁰ C	$\alpha+\beta+x_2+x_3$	-	$\alpha+\beta+x_2+x_3$	$\alpha+\beta+x_2+x_3$
10 ⁰ C/min, 1700 ⁰ C, 1 h.	$\alpha+\beta+x_2+x_3$	$\alpha+\beta+x_2+x_3$	$\alpha+\beta+x_2+x_3$	$\alpha+\beta+x_2+x_3$
10 ⁰ C/min, 1700 ⁰ C, 2 h.	$\alpha+\beta+X_2+x_3$	$\alpha+\beta+X_2+x_3$	$\alpha+\beta+X_2+x_3$	$\alpha+\beta+X_2+x_3$

Note: $X_2 = Si_2N_2O$

X_3 = Unknown

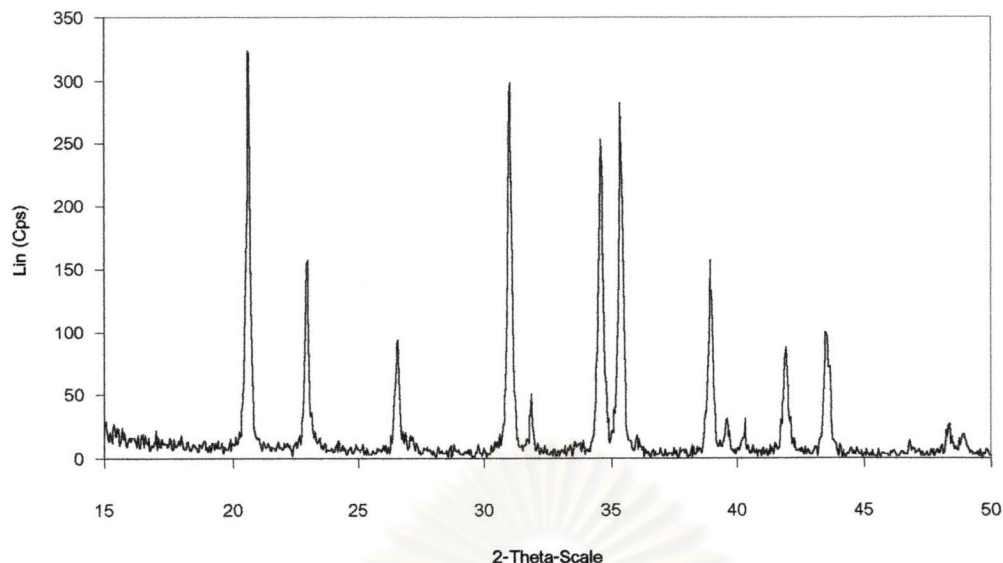


Fig E-1 X-ray diffraction pattern of the SN-E10 packing powder raw material

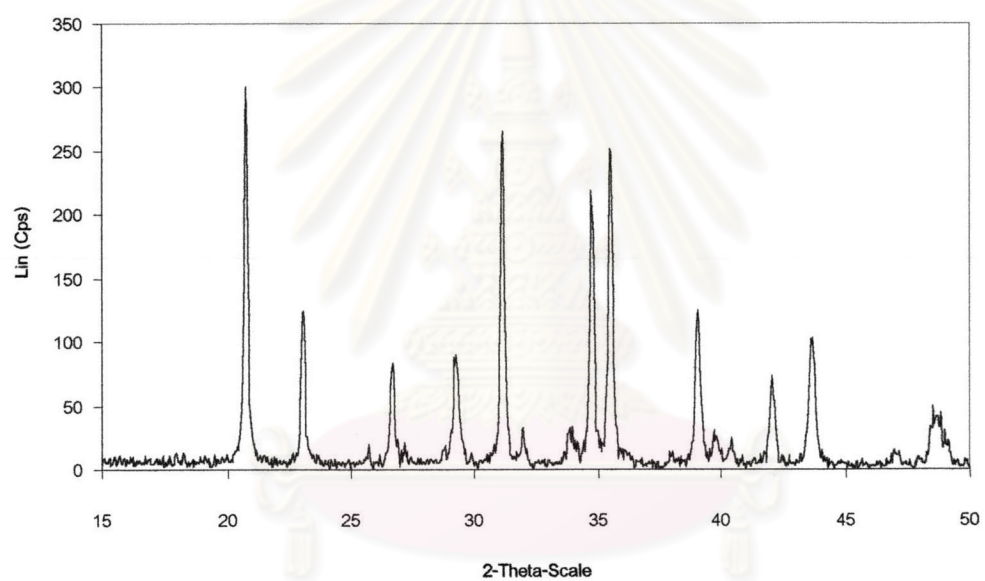


Fig E-2 X-ray diffraction pattern of the Mix powder A raw material

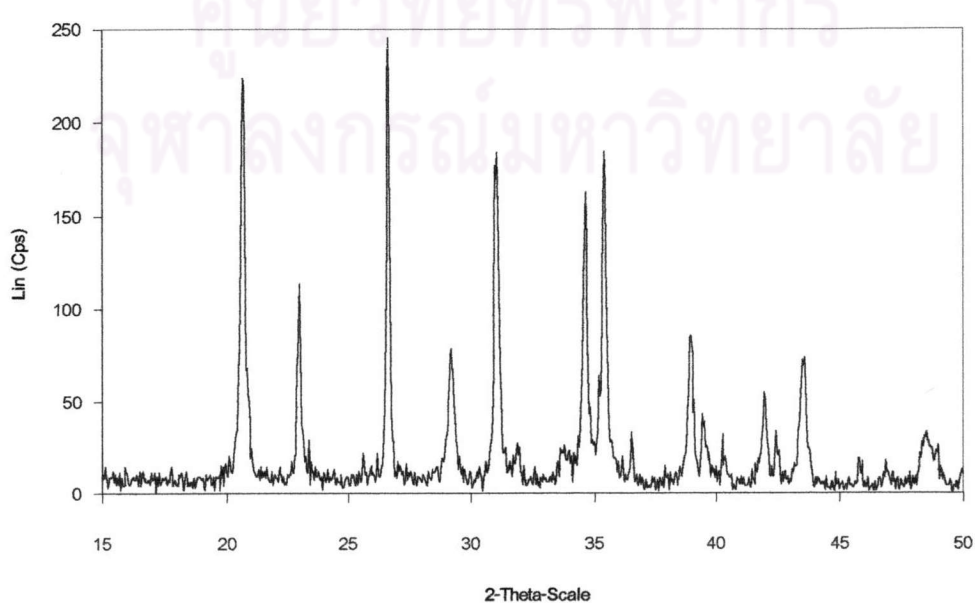


Fig E-3 X-ray diffraction pattern of Mix powder B raw material

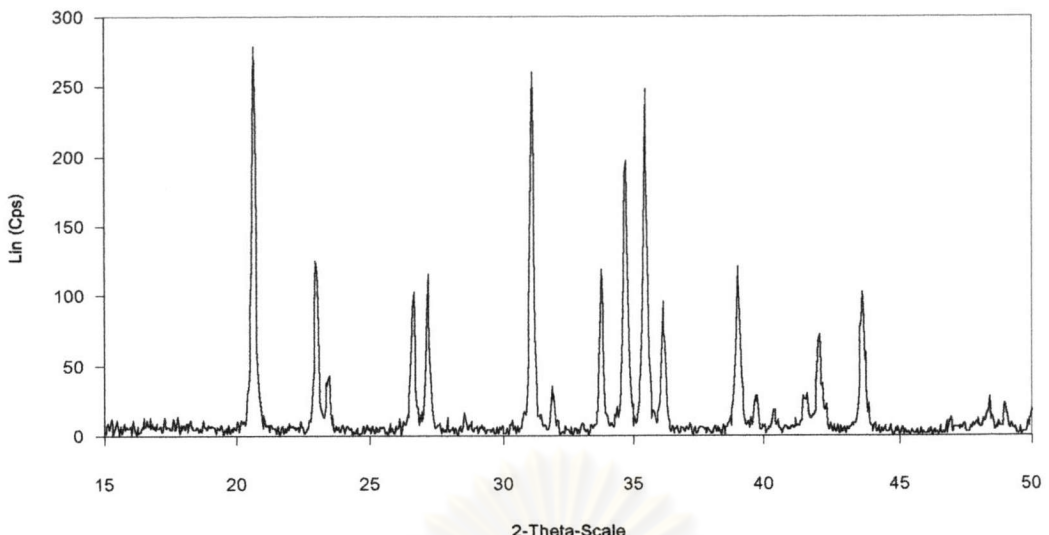


Fig E-4 X-ray diffraction of the SN-7 packing powder raw material

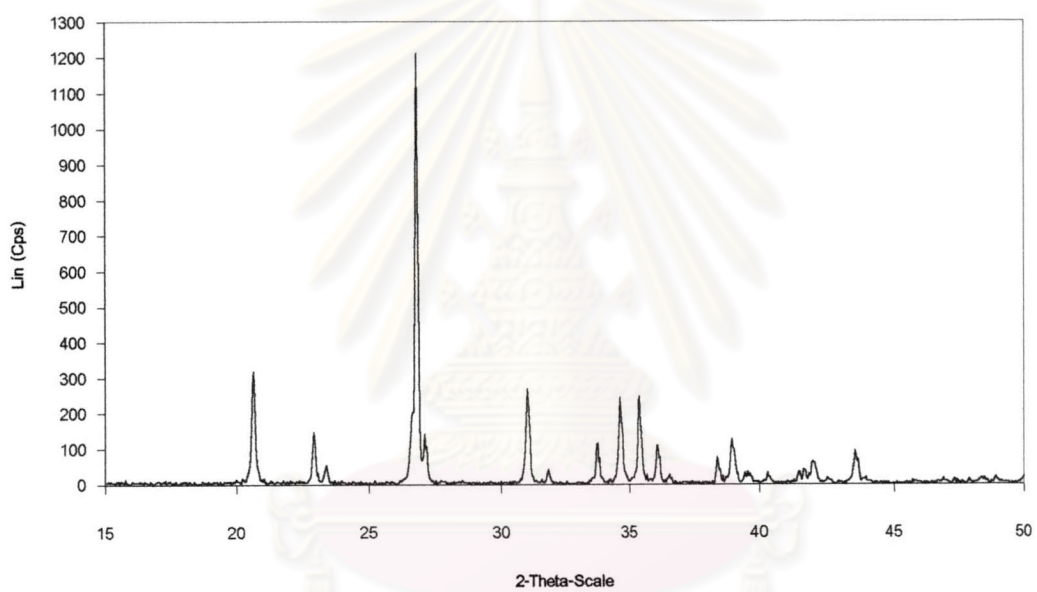


Fig E-5 X-ray diffraction of the SN-7+10 mass % BN packing powder raw material

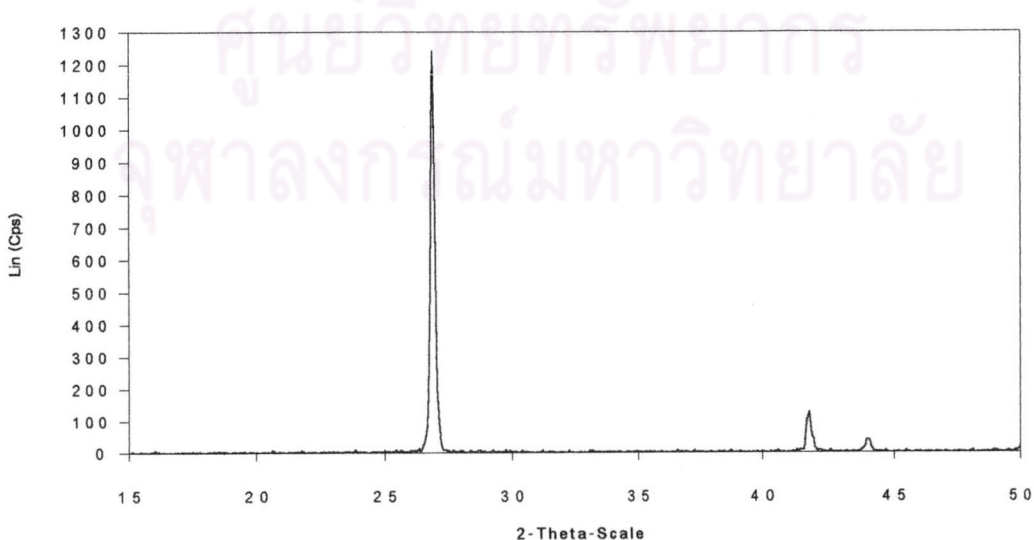


Fig E-6 X-ray diffraction pattern of boron nitride raw material

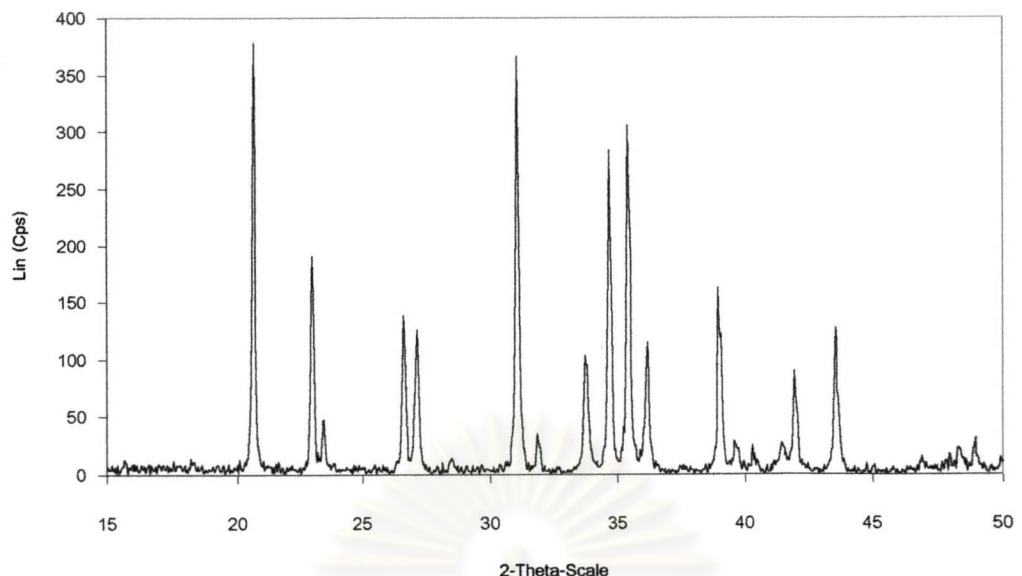


Fig E-7 X-ray diffraction pattern of SN-KO5 packing powder raw material

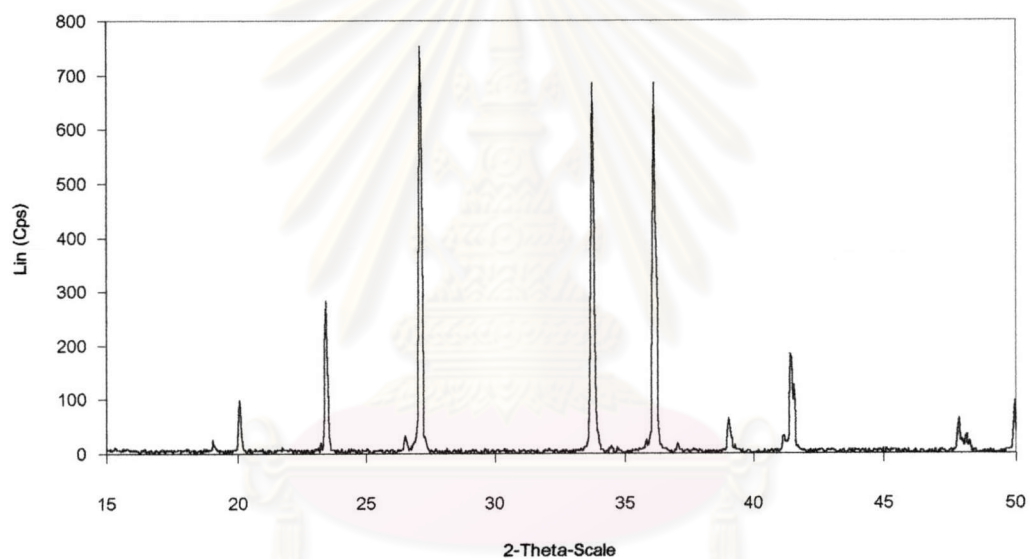


Fig E-8 X-ray diffraction pattern of SN-F2 packing powder raw material

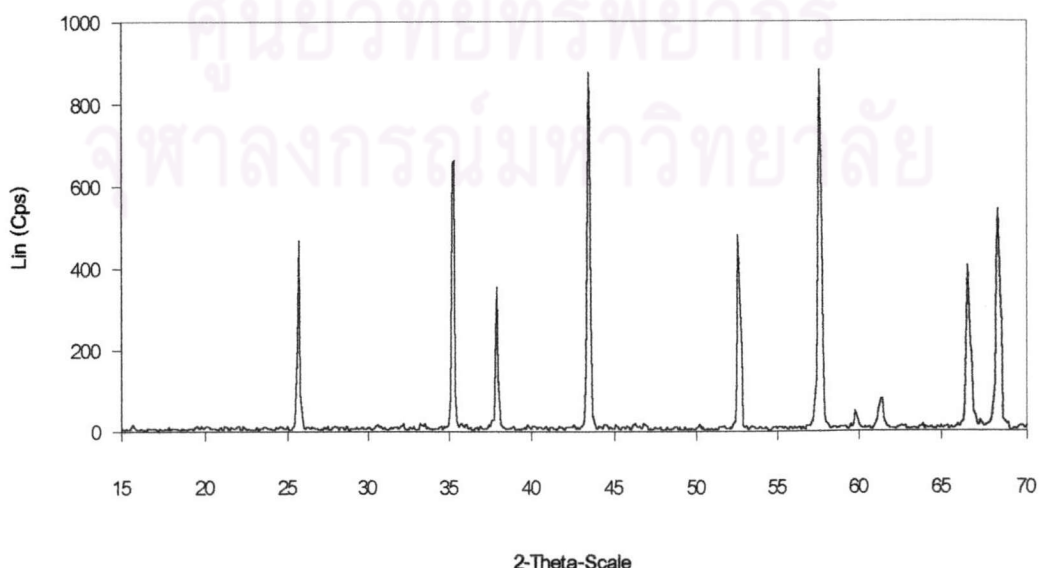
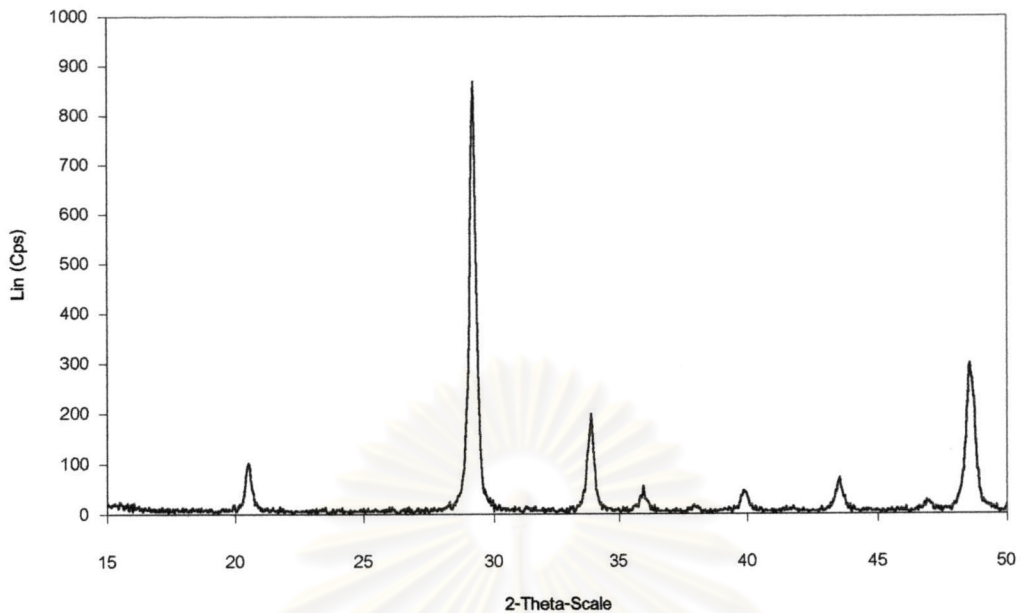
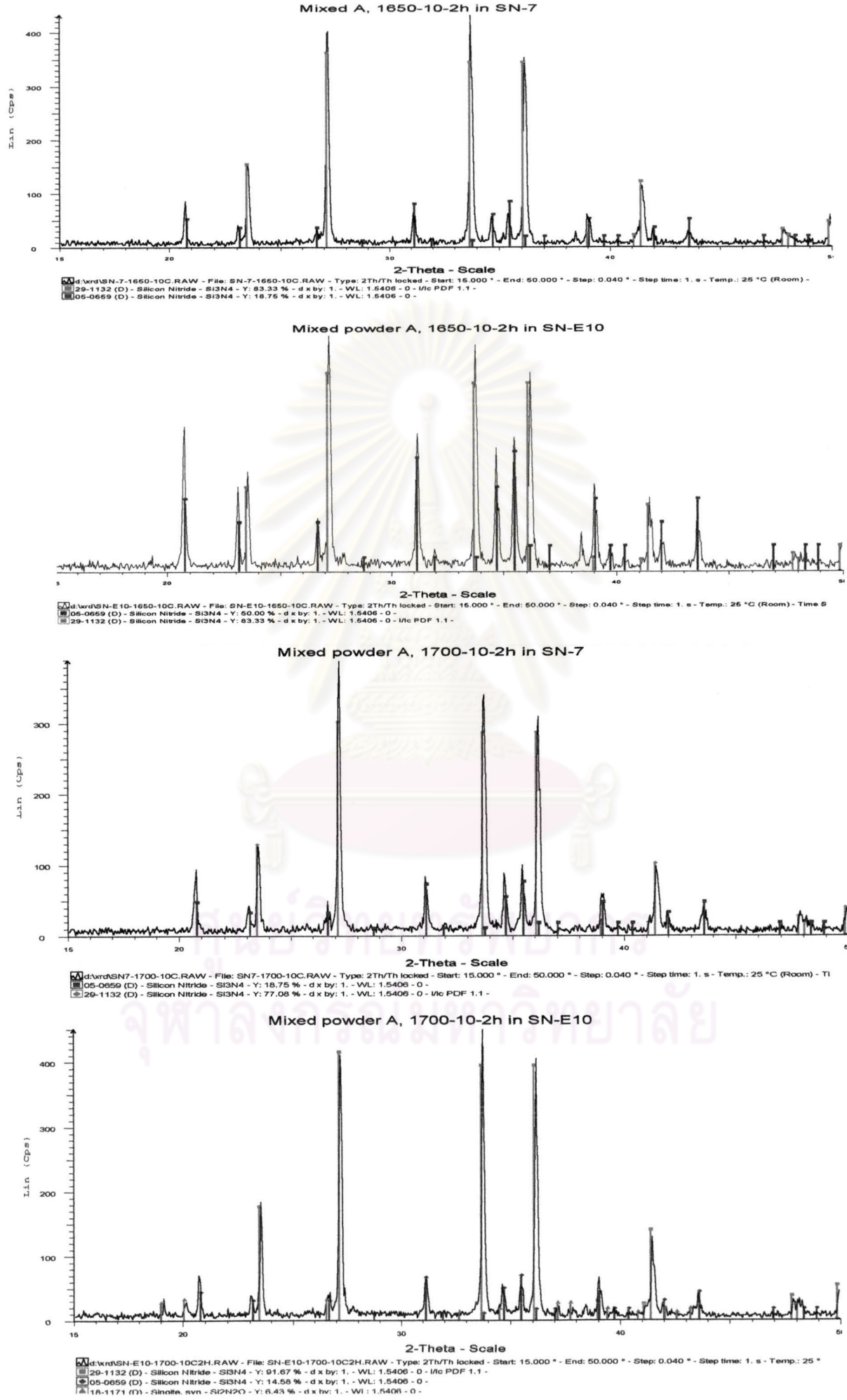


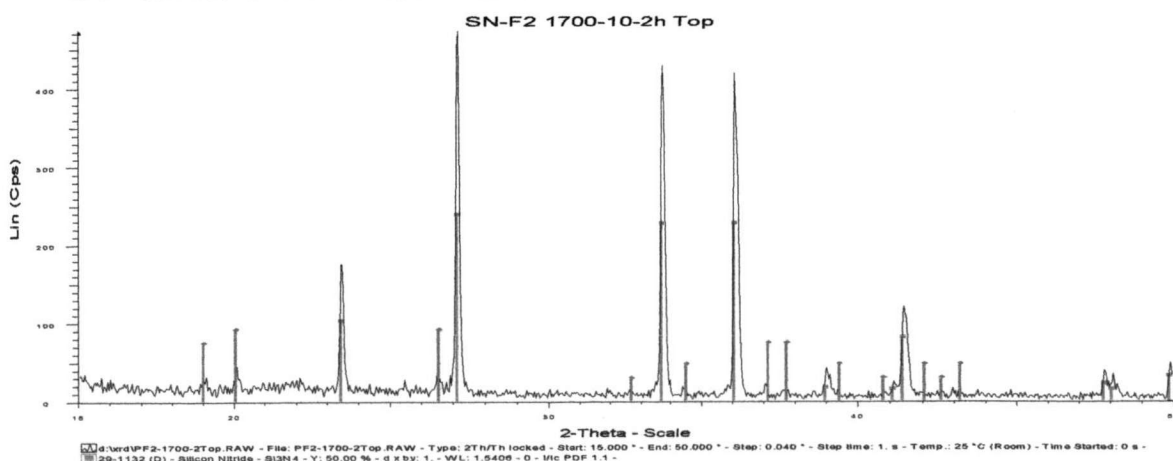
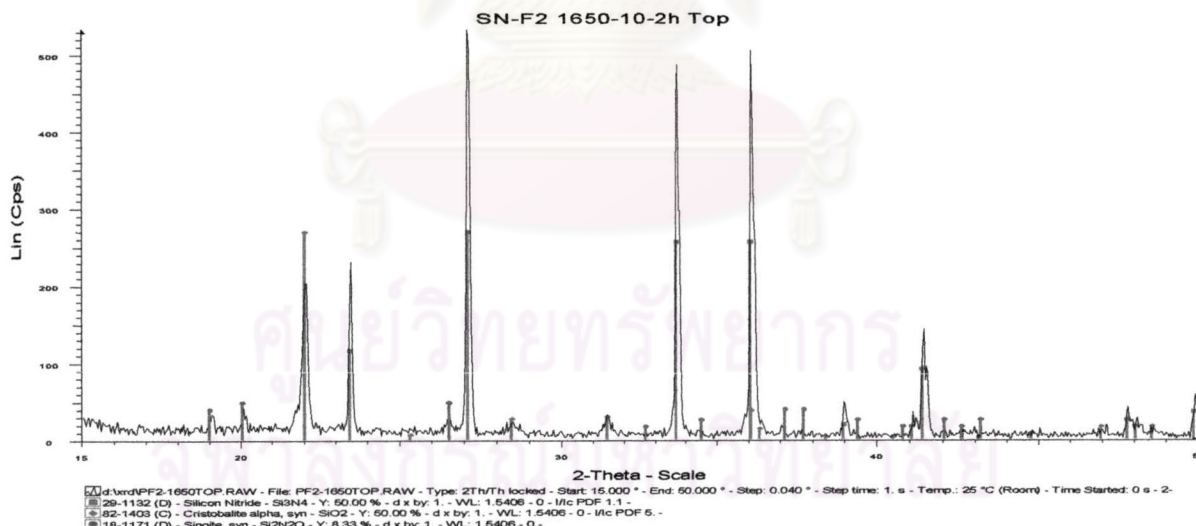
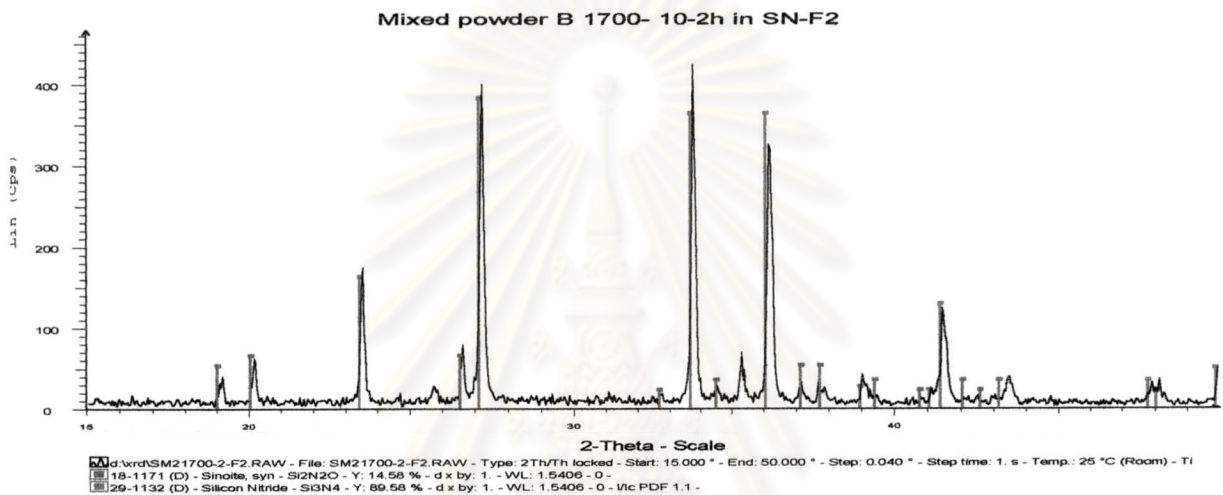
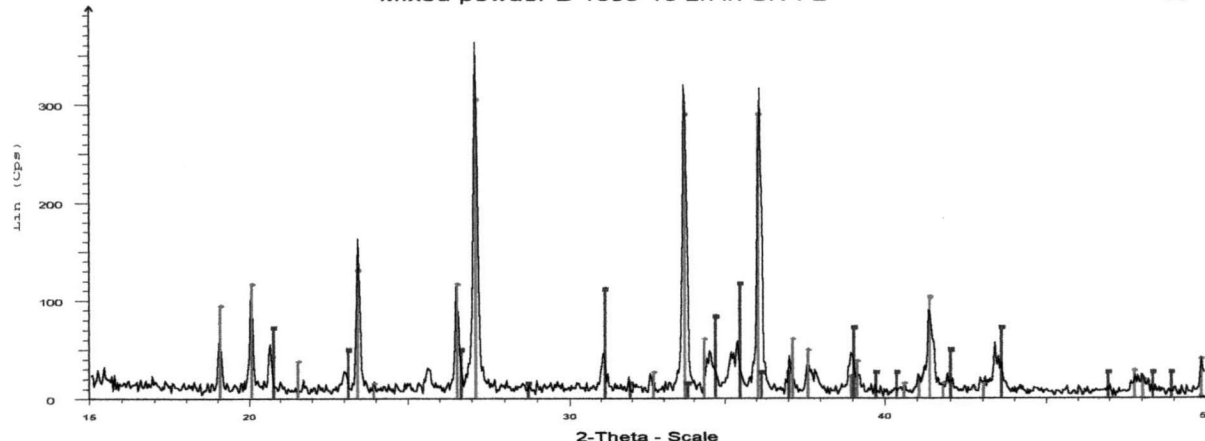
Fig E-9 X-ray diffraction pattern of A-11 packing powder after sintering



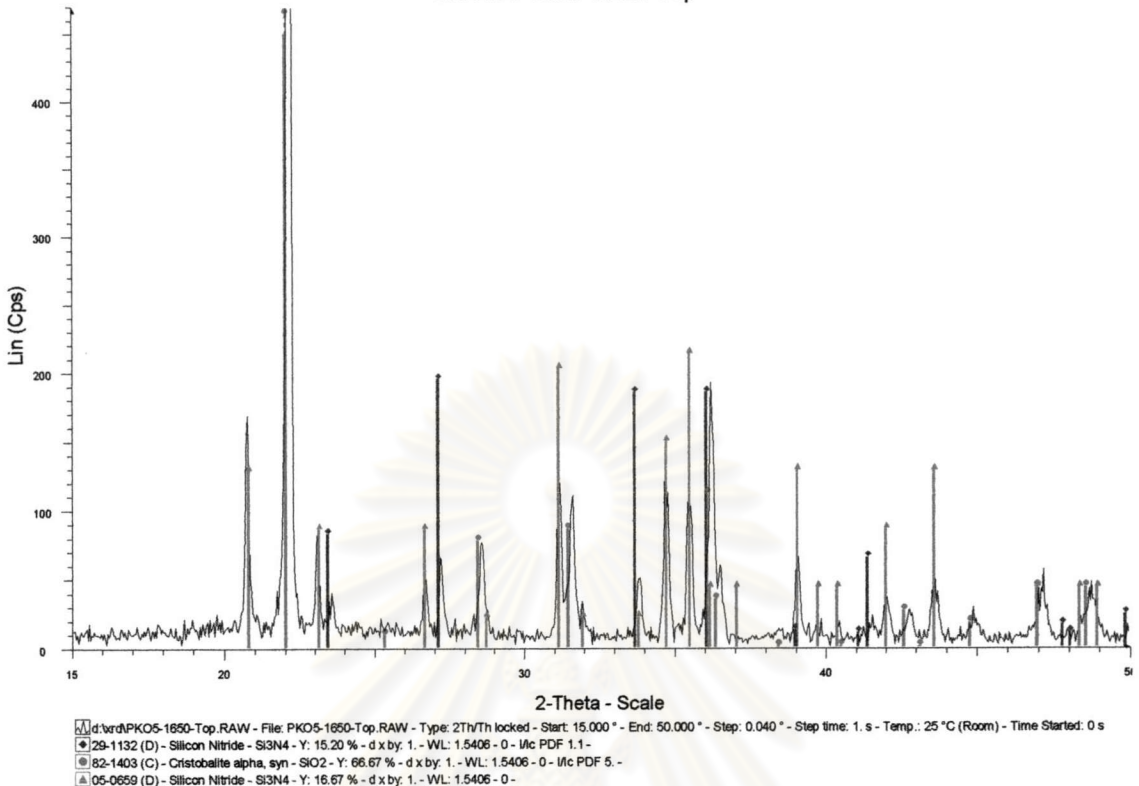
Appendix E-10 X-ray diffraction pattern of Y_2O_3 raw material

ศูนย์วิทยทรัพยากร
จุฬาลงกรณ์มหาวิทยาลัย

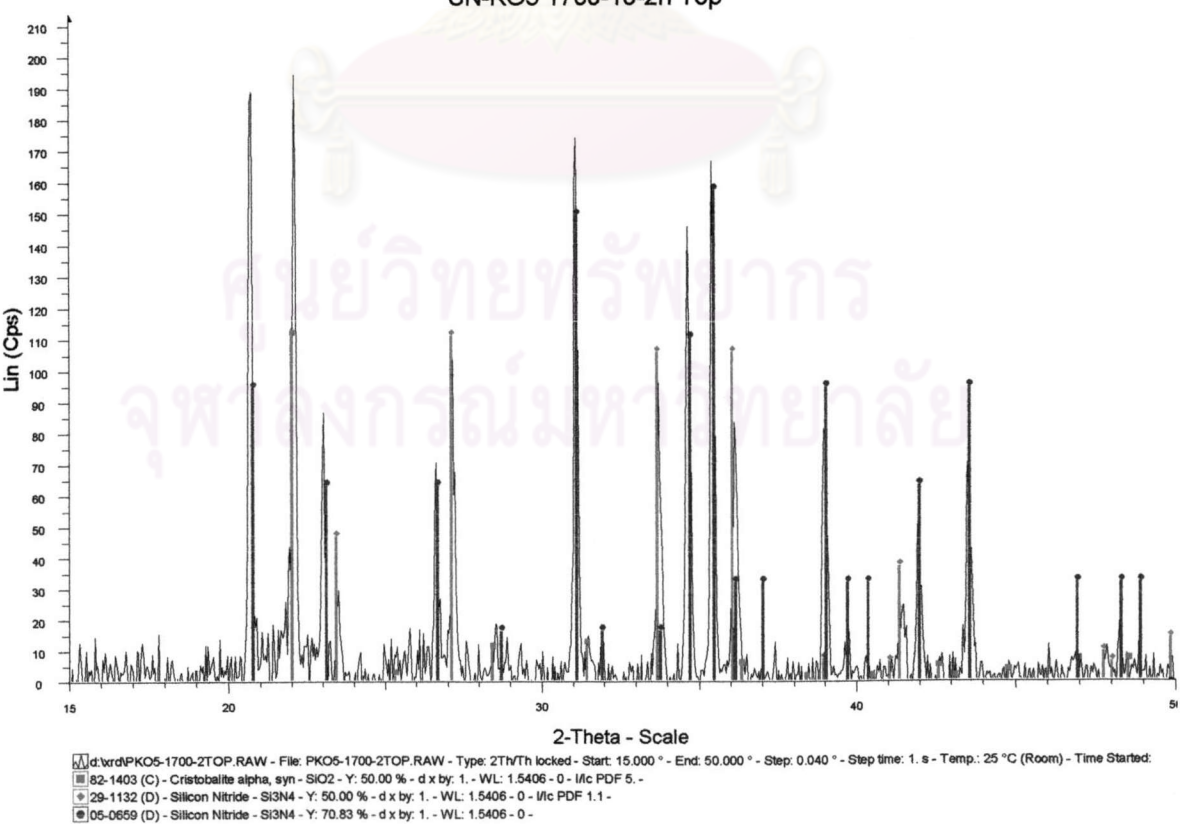


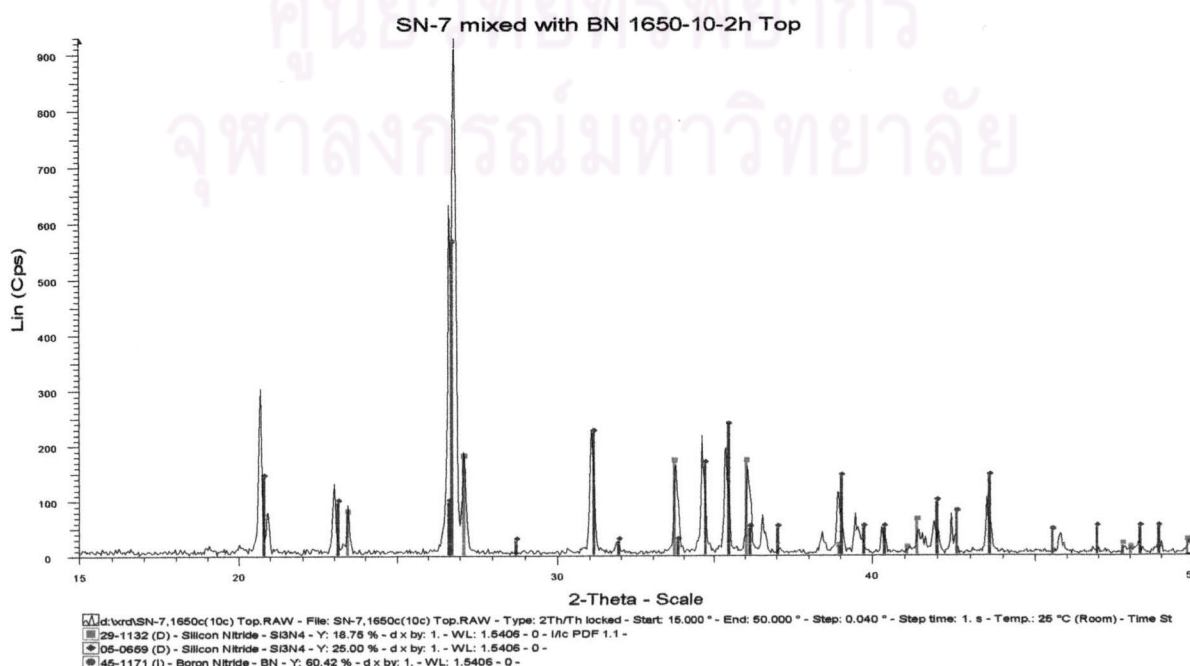
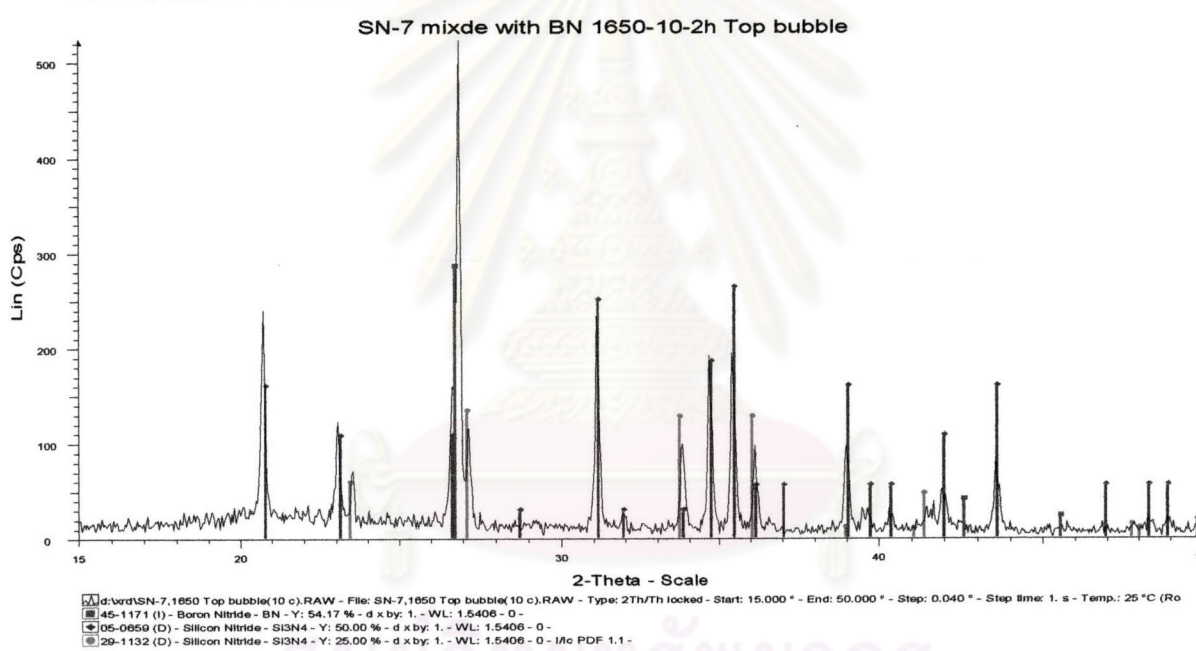
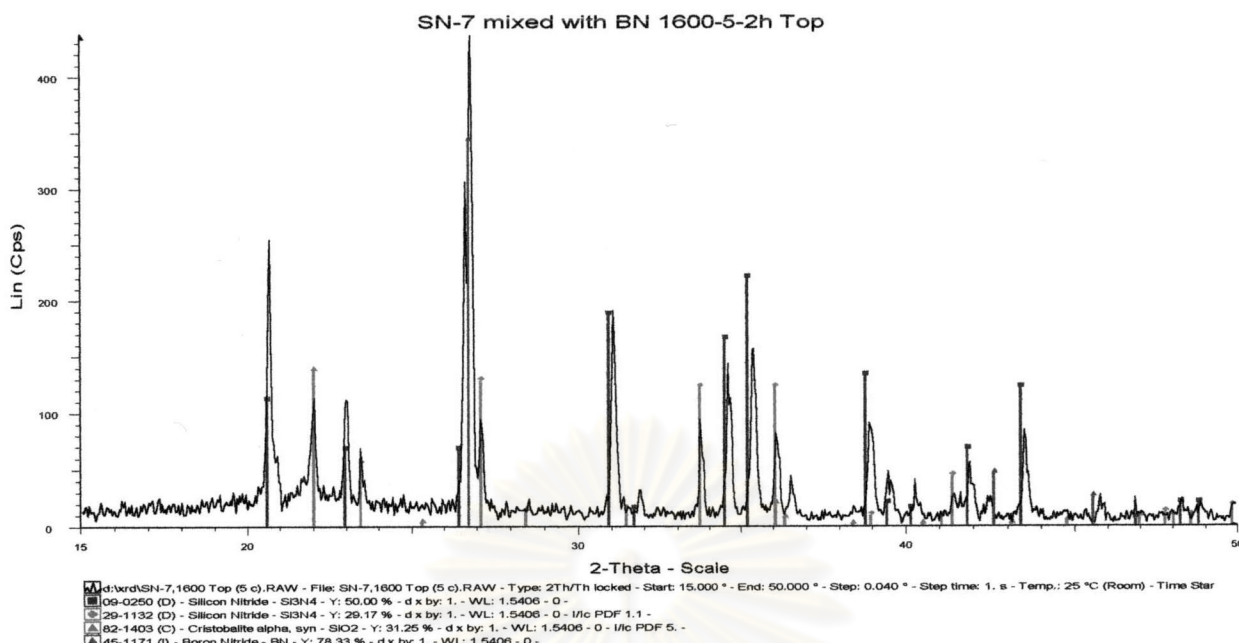


SN-KO5 1650-10-2h Top

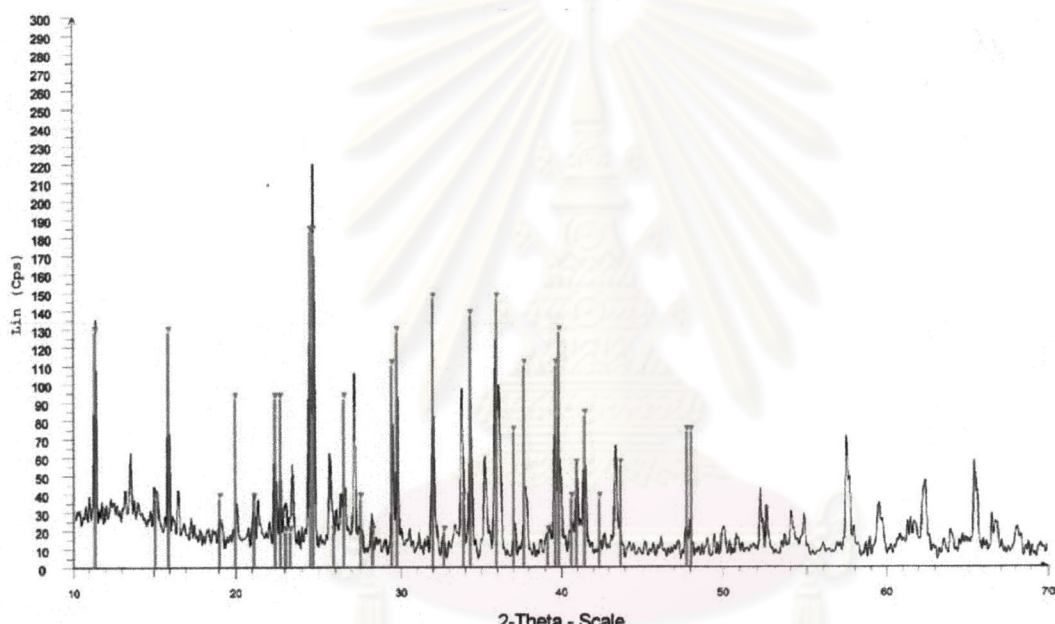
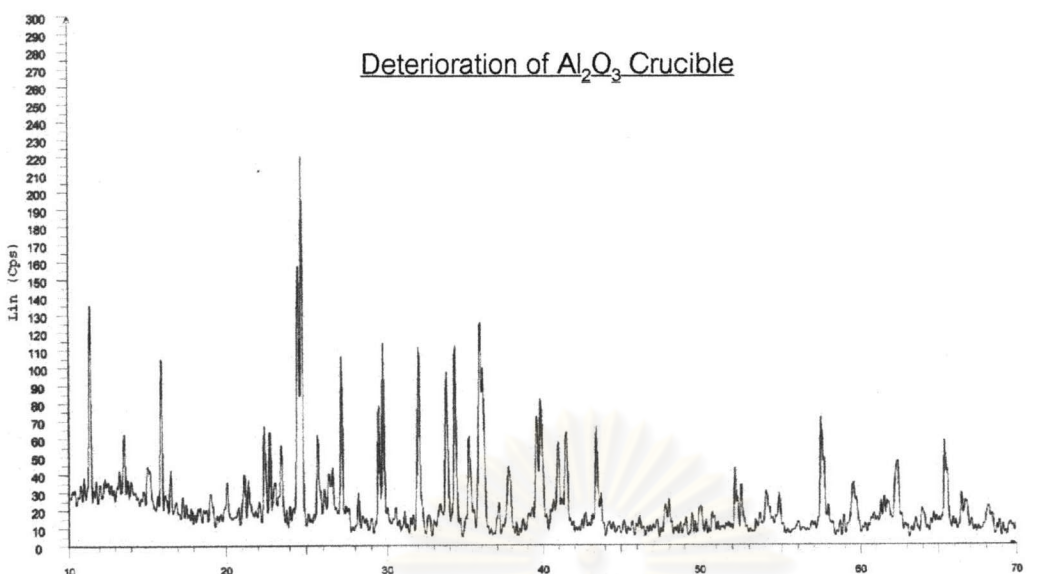


SN-KO5 1700-10-2h Top



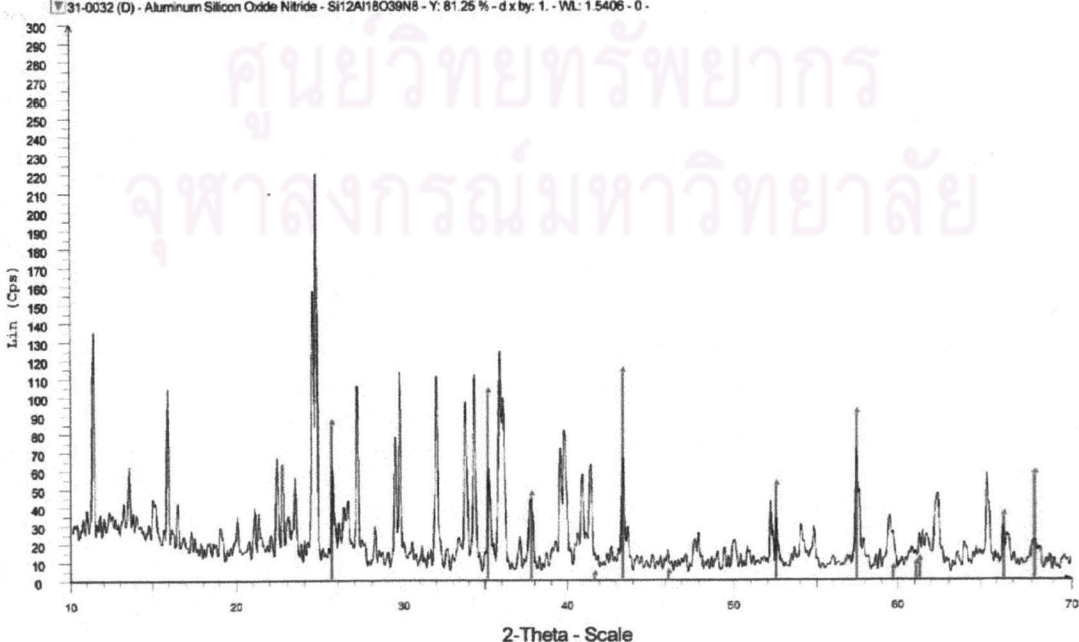


Deterioration of Al₂O₃ Crucible



2-Theta - Scale

d:\wrdNS1.RAW - File: ls1.raw - Type: 2Th/Th locked - Start: 10.000 ° - End: 70.000 ° - Step: 0.050 ° - Step time: 1. s - Temp.: 25 °C (Room) - Time Started: 0 s - 2-Theta:
 31-0032 (D) - Aluminum Silicon Nitride - Si₁2Al₁₈O₃₉N₈ - Y: 81.25 % - d x by: 1. - WL: 1.5406 - 0 -



2-Theta - Scale

d:\wrdNS1.RAW - File: ls1.raw - Type: 2Th/Th locked - Start: 10.000 ° - End: 70.000 ° - Step: 0.050 ° - Step time: 1. s - Temp.: 25 °C (Room) - Time Started: 0 s - 2-Theta:
 10-0173 (I) - Corundum, syn - Al₂O₃ - Y: 50.00 % - d x by: 1. - WL: 1.5406 - 0 - IIC PDF 1. -

APPENDIX F

Table F-1 Results of fracture toughness (K_{IC}) and Vickers hardness (HV) of sintered specimens at 1700 °C. (Crack length was measured by SEM)

Conditions (Soaking time)	Sample No. (Piece)	c (μm)	A (μm)	K_{IC} (MPa . m ⁽¹⁻²⁾)	HV (GPa)
1 h	1	95.60	51.45	4.90	17.16
	2	88.20	52.95	5.18	16.22
	3	126.50	50.00	4.33	18.18
	4	120.60	50.00	4.40	18.18
	5	123.50	51.45	4.50	17.16
Average				4.66	17.38
2 h	1	102.90	54.40	5.05	15.35
	2	97.10	54.40	5.15	15.35
	3	97.10	52.95	5.01	16.24
	4	105.90	52.95	4.87	16.24
	5	102.90	52.95	4.91	16.24
Average				5.00	15.88

Table F-2 Results of fracture toughness (K_{IC}) and Vickers hardness (Hv) of sintered specimens at 1700 °C. (Crack length was measured by Optical microscope, OM)

Conditions (Soaking time)	Sample No. (Piece)	c (μm)	a (μm)	K_{IC} ($\text{MPa} \cdot \text{m}^{(1-2)}$)	HV (GPa)
1 h	1	93.20	51.40	5.29	17.21
	2	102.30	53.50	5.13	15.88
	3	108.90	51.40	5.05	17.21
	4	90.40	52.30	5.40	16.62
	5	105.00	53.50	4.99	15.88
Average				5.17	16.56
2 h	1	85.00	54.80	5.47	15.14
	2	93.70	54.30	4.90	15.42
	3	96.40	53.60	5.07	15.82
	4	96.20	52.90	5.24	16.25
	5	97.40	53.20	5.01	16.06
Average				5.13	15.74

Note: Scale 1 mm = 20 μm

ศูนย์วิทยทรัพยากร
จุฬาลงกรณ์มหาวิทยาลัย

Table F-3 Calculation results of flexural strength, S.

Lot of powder B	Sample No. (Piece)	Diameter, c (mm)	Thickness, d (mm)	P (N)	S (MPa)
Lot 3	1	2.71	1.48	762.00	487.26
	2	2.71	1.48	715.80	457.72
	3	2.71	1.48	791.40	506.06
	4	2.71	1.48	577.20	369.09
	5	2.71	1.48	542.60	346.97
	6	2.73	1.47	678.80	434.06
	7	2.71	1.46	608.10	388.85
Average					427.14
Lot 4	1	2.73	1.44	621.20	397.23
	2	2.71	1.48	740.20	473.32
	3	2.71	1.48	582.90	372.74
	4	2.73	1.51	391.00	250.03
	5	2.71	1.49	730.50	467.12
	6	2.71	1.50	684.00	437.38
	7	2.70	1.49	530.60	339.29
Average					414.51

**ศูนย์วิทยทรัพยากร
จุฬาลงกรณ์มหาวิทยาลัย**

Appendix G

Properties of TOSHIBA's specimen (standard bars)

1. Chemical composition

Composition (mass %)			
Si_3N_4	Y_2O_3	Al_2O_3	TiO_2
89.5	4.5	5.0	1.0

2. Estimated real density:

3.31 g/cm³

The calculation was performed assuming that 1 % of Si_3N_4 is oxygen. Then, the contents of Si_3N_4 and SiO_2 are 87.82 g and 1.67 g, respectively. Densities of SiO_2 , Y_2O_3 , Al_2O_3 , TiO_2 and Si_3N_4 are 2.20, 4.84, 4.00, 4.25 and 3.21 g/cm³, respective.

3. Bulk density and relative density

Measured bulk density was 3.19 g/cm³. Then, relative density is 96.4 %

4. Vickers' Hardness

16.0 GPa

5. Fracture Toughness

Crack length was measured by optical microscope. K_{1C} was calculated by two equations.

Crack	K_{1C} (MPa.m ^{1/2})
Median crack	5.0
Palmqvist crack	5.9

$$K_{1C} = 0.026 \{E^{1/2} P^{1/2} (a/c)^{-3/2}\} \quad \text{for Median cracks}$$

$$K_{1C} = 0.018 H(a^{1/2})(E/H^{0.4})\{(c/a)-1\}^{-1/2} \quad \text{for Median cracks}$$

Young's Modulus, E = 280 GPa.

BIOGRAPHY

Miss. Piyaporn Chaiyapuck was born in Sisaket on 12th of July 1977. She was received a Bachelor Degree in Ceramic Engineering from Faculty of Engineer, Suranaree University in 2000. After graduating, she worked at Casday Co. Ltd. for a year and continued study in Master Degree in the field of Ceramic Technology at Chulalongkorn University and graduated in June 2003.

ศูนย์วิทยทรัพยากร
จุฬาลงกรณ์มหาวิทยาลัย